# Immobilizing the Moving Parts of Voltage-gated Ion Channels

Richard Horn,* Shinghua Ding,* and Hermann J. Gruber‡

From the *Department of Physiology, Jefferson Medical College, Philadelphia, Pennsylvania 19107; and ‡Institute of Biophysics, Johannes Kepler University, A-4040 Linz, Austria

abstract Voltage-gated ion channels have at least two classes of moving parts, voltage sensors that respond to changes in the transmembrane potential and gates that create or deny permeant ions access to the conduction pathway. To explore the coupling between voltage sensors and gates, we have systematically immobilized each using a bifunctional photoactivatable cross-linker, benzophenone-4-carboxamidocysteine methanethiosulfonate, that can be tethered to cysteines introduced into the channel protein by mutagenesis. To validate the method, we first tested it on the inactivation gate of the sodium channel. The benzophenone-labeled inactivation gate of the sodium channel can be trapped selectively either in an open or closed state by ultraviolet irradiation at either a hyperpolarized or depolarized voltage, respectively. To verify that ultraviolet light can immobilize S4 segments, we examined its relative effects on ionic and gating currents in *Shaker* potassium channels, labeled at residue 359 at the extracellular end of the S4 segment. As predicted by the tetrameric stoichiometry of these potassium channels, ultraviolet irradiation reduces ionic current by approximately the fourth power of the gating current reduction, suggesting little cooperativity between the movements of individual S4 segments. Photocross-linking occurs preferably at hyperpolarized voltages after labeling residue 359, suggesting that depolarization moves the benzophenone adduct out of a restricted environment. Immobilization of the S4 segment of the second domain of sodium channels prevents channels from opening. By contrast, photocross-linking the S4 segment of the fourth domain of the sodium channel has effects on both activation and inactivation. Our results indicate that specific voltage sensors of the sodium channel play unique roles in gating, and suggest that movement of one voltage sensor, the S4 segment of domain 4, is at least a two-step process, each step coupled to a different gate.

key words: cysteine mutagenesis • sodium channel • *Shaker* potassium channel • benzophenone • S4 segment

## INTRODUCTION

Voltage-dependent gating of ion channels typically involves two types of physically distinct participants, voltage sensors that move in response to changes of membrane potential, and gates that control access to the permeation pathway (Sigworth, 1994; Yellen, 1998; Bezanilla, 2000). Although there are excellent candidates for each in specific regions of the channel protein, little is known about how the movement of one affects the conformation of the other. To begin to tackle this problem, we have developed a new approach, the systematic immobilization of the moving parts of the channel using a combination of cysteine mutagenesis and a photoactivatable cross-linker that can be tethered covalently to the introduced cysteines. We then examine the biophysical consequences of immobilizing either voltage sensors or gates by exposing the labeled channels to ultraviolet light.

The voltage-dependent channels selective for either sodium, calcium, or potassium ions have an approximately fourfold radial symmetry with each domain, or subunit, containing six putative transmembrane segments, S1–S6. The main voltage sensors are the four positively charged S4 segments. Each S4 segment has two to eight basic residues, either arginines or lysines, which are usually separated from each other by two neutral residues. Depolarization is expected to move S4 segments outward through the electric field (Catterall, 1986; Sigworth, 1994; Keynes, 1994; Yellen, 1998; Keynes and Elinder, 1999; Bezanilla, 2000). The initial effect of this S4 movement is the opening of the activation gate, believed to be located near the cytoplasmic end of the channel's four S6 segments, at the entrance of the permeation pathway (Holmgren et al., 1997; Liu et al., 1997; Del Camino et al., 2000). Prolonged depolarization also causes the inactivation gates to close.

Our results show that (a) the inactivation gate of the sodium channel can be immobilized selectively in either an open or closed conformation, (b) immobilization of a single S4 segment of a *Shaker* potassium channel has little effect on the movements of other S4 segments of the channel, and (c) the consequence of immobilizing a sodium channel S4 segment depends not only on the domain of its origin, but also on whether the cross-linker is attached to the extracellular or cytoplasmic side of the protein. The data suggest that individual movements of the S4 segment of domain 4 of the sodium channel are coupled to different gates.

Address correspondence to Richard Horn, Department of Physiology, Jefferson Medical College, 1020 Locust Street, Philadelphia, PA 19107. Fax: 215-503-2073; E-mail: Richard.horn@mail.tju.edu

## METHODS

### *Mutants and Transfection*

Cysteine mutants of sodium channels were constructed in the human skeletal muscle sodium channel (hSKM1). The cysteine mutant of isoleucine$^{1310}$ (IFM/CFM mutant)[1] in the cytoplasmic linker connecting domains 3 and 4 was a gift from Dr. M. Chahine (Laval University, Quebec, Canada), and Dr. A.L. George (Vanderbilt University, Nashville, TN) contributed other sodium channel mutants. The expression vector for sodium channels was pRc/CMV (Invitrogen).

Dr. A. Melishchuk (University of Pennsylvania, Philadelphia, PA) provided the *Shaker*-IR (a construct of *Shaker* in which part of the amino terminus is removed to abolish N-type inactivation) potassium channel cDNA in the pGW1-CMV vector (British Biotechnology). The *Shaker*-IR variant we obtained lacked residues 6–46 to remove N-type inactivation and also had the point mutation Thr449→Val to partially inhibit C-type inactivation (Melishchuk et al., 1998). We made the Ala359→Cys point mutation using the QuikChange™ Site-Directed Mutagenesis Kit (Stratagene). The mutagenic primers for this A359C mutant were 5′-CAG GCT ATG TCC TTG TGC ATA TTA CGA GTG ATA CG-3′ and 5′-CGT ATC ACT CGT AAT ATG CAC AAG GAC ATA GCC TG-3′. The mutation was confirmed by sequencing to exclude polymerase errors.

The tsA201 cells, which are transformed HEK293 cells, were transfected using a standard calcium phosphate method. After 6–12 h, the transfected cells were passed onto 25-mm round, 1-mm thick glass coverslips, each of which formed the bottom of a chamber mounted on the stage of an inverted compound microscope (TE-300 Eclipse; Nikon).

### *Electrophysiology and Data Acquisition*

Standard whole-cell recording methods were used (Yang and Horn, 1995). Patch electrodes contained (mM): 105 CsF, 35 NaCl, 10 EGTA, 10 Cs-HEPES, pH 7.4. The bath contained 150 NaCl, 2 KCl, 1.5 $CaCl_2$, 1 $MgCl_2$, 10 Cs-HEPES, pH 7.4. For recording from *Shaker* potassium channels, the patch electrodes contained 140 NMDG, 100 HF, 6 CsCl, 5 EGTA, 10 HEPES, pH titrated to 7.3 with methanesulfonic acid; and the bath contained 140 NMDG, 70 methanesulfonic acid, 30 CsCl, 1 $CaCl_2$, 1 $MgCl_2$, 10 HEPES, pH titrated to 7.4 with HCl. The patch-clamp amplifier was an Axopatch 200B (Axon Instruments, Inc.). Corrections were made for liquid junction potentials. Series resistance was usually $<3$ MΩ, and voltage errors were $<3$ mV after compensation. Data were filtered at 5–10 kHz and acquired using Clampex 8.0 (Axon Instruments, Inc.). Gating currents for *Shaker*-IR channels were obtained using P/$-8$ correction pulses for capacitance and leakage in a voltage range more hyperpolarized than $-120$ mV. Whole-cell data were displayed and analyzed by a combination of pCLAMP programs (Axon Instruments, Inc.), EXCEL (Microsoft Corp.), ORIGIN (MicroCal), and our own FORTRAN programs. Experiments were done at room temperature (20–22°C). Data from at least three cells for each measurement are presented as mean ± SEM.

### *Reagent*

Benzophenone-4-carboxamidocysteine methanethiosulfonate (BPMTS) was a custom synthesis by Toronto Research Chemicals. A 100-mM stock of BPMTS in ethyl acetate was stored at 4°C for up to 1 wk and diluted into either bath or pipette solution immediately before use. Extracellular labeling of cysteines was done by treating a coverslip of attached cells with 1 mM BPMTS for 10 min. For *Shaker* and the D2:R1C mutant, we added 50 mM KCl to the bath solution during labeling to depolarize the cells and expose all S4 segments to the reagent. Up to 1 mM BPMTS was added to the patch pipette for cytoplasmic labeling.

### *Photocross-linking*

Benzophenone was photoactivated by UV light presented to a voltage-clamped cell through a 40× (1.3 N.A.) oil immersion objective (S Fluor; Nikon). The UV light source was either a continuously operating 75-watt xenon-arc lamp interrupted by a mechanical shutter (IonOptix) or a FlashMic xenon flashlamp with an ∼580 μs full width at half magnitude pulse (Rapp OptoElectronic) triggered by the data acquisition system. For the experiments in this study, equivalent results were obtained with both methods of irradiation. Light was bandpass filtered between 340 and 380 nm to reduce photodamage and heat.

## RESULTS

To immobilize specific regions of ion channels, we attached a photoactivatable cross-linking group to cysteine residues substituted into these regions, and irradiated them with UV light. Fig. 1 shows the bifunctional reagent we designed for this purpose, BPMTS. The thiolate group of a cysteine sidechain of the channel protein will attack the methanethiosulfonate group of the reagent (curved arrow), resulting in the covalent attachment of the benzophenone (diaryl ketone) moiety to the cysteine residue. Because BPMTS has a net negative charge, due to the carboxylate anion in the linker, the reagent cannot readily cross the membrane and will tend to label cysteines on the surface of the channel protein. Absorption by benzophenone of a photon at a wavelength of ∼350 nm generates a triplet excited state, promoting the insertion of the ketone into neighboring C-H bonds, especially those in the peptide backbone (Dormán and Prestwich, 1994). The efficiency of this insertion depends on the local environment of the insertion site, but can attain levels of >70%. Thus, UV irradiation will tend to cross-link a cysteine labeled with BPMTS to adjacent regions of the channel protein.

We initially tested this experimental method on a gate, because of the simplicity of the predicted results. We expected to be able to immobilize a BPMTS-labeled gate either open or closed, depending on when UV light was applied. We chose the fast inactivation gate of the sodium channel, postulated to be the cytoplasmic linker between domains 3 and 4 (Patton et al., 1992; West et al., 1992), for this test. Three consecutive residues in the middle of this linker play a critical role in fast inactivation, isoleucine-phenylalanine-methionine (IFM). We used a mutant (IFM/CFM) in which the isoleucine was replaced by cysteine, and labeled this cysteine with BPMTS by placing the reagent (at 62.5 μM) in the patch pipette during whole cell recording. The slowing of inactivation (Fig. 2, A and B) caused by the reagent is evidence for the covalent modification of

[1]*Abbreviations used in this paper:* BPMTS, benzophenone-4-carboxamidocysteine methanethiosulfonate; IFM, isoleucine$^{1310}$-phenylalanine$^{1311}$-methionine$^{1312}$; IFM/CFM, cysteine mutant of isoleucine$^{1310}$.

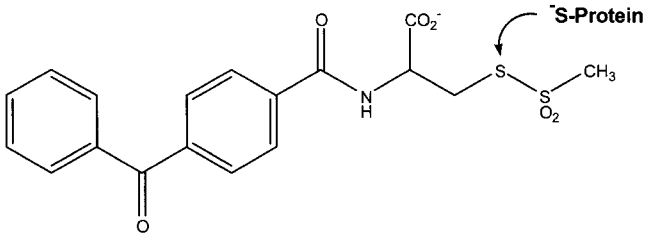


Figure 1. BPMTS. The arrow shows where the cysteine thiolate attacks the reagent, leading to a covalent linkage by a disulfide bond.

the cysteine (Kellenberger et al., 1996; Deschênes et al., 1999). No effect on inactivation was observed in wild-type channels with a similar exposure to either internal or external BPMTS at the highest concentration (1 mM) used in this study (data not shown).

We then tested whether the mutant with a labeled inactivation gate (IFM/CFM-BP) could be trapped selectively in an open or closed conformation. UV irradiation with a 75-watt continuous-power xenon lamp at a hyperpolarized (−140 mV) voltage, where the inactivation gate should be open, had two effects (Fig. 2 C). The main effect was a reduction in the fraction of channels that inactivated during a −20-mV test pulse from 0.94 to 0.55; however, it also caused a 7.5% reduction of the peak current. This reduction might be due to a small fraction of channels whose inactivation gates were immobilized shut at −140 mV. The channels that continued to inactivate did so at the same rate as before irradiation (for details, see Fig. 2, legend), suggesting that their benzophenone groups had not effectively inserted in response to UV. Subsequent exposure to UV had no further effect on the currents of this cell (data not shown). If the UV light was applied at 0 mV (Fig. 2 D), where the inactivation gates are primarily closed, the main effect was a 51.9% reduction of peak current with less effect on the residual current, suggesting that inactivation gates were mainly trapped shut. Again, there was no effect of irradiation on the time constant of inactivation for channels that continued to inactivate. Similar results were obtained in 16 other cells irradiated at the holding potential and five other cells irradiated at 0 mV.

These experiments verify that a moving part, the inactivation gate, can be immobilized selectively in either an open or closed conformation, lending credence to the use of this technique for another moving part, the S4 voltage sensor. Moreover, these results provide support for the hinged lid model of inactivation (West et al., 1992).

*Immobilization of S4 Segments in Shaker*

To test whether BP-labeled S4 segments can be immobilized by UV irradiation, we turned to measurements of gating and ionic current in a cysteine mutant of *Shaker* potassium channels. The rationale for this choice was

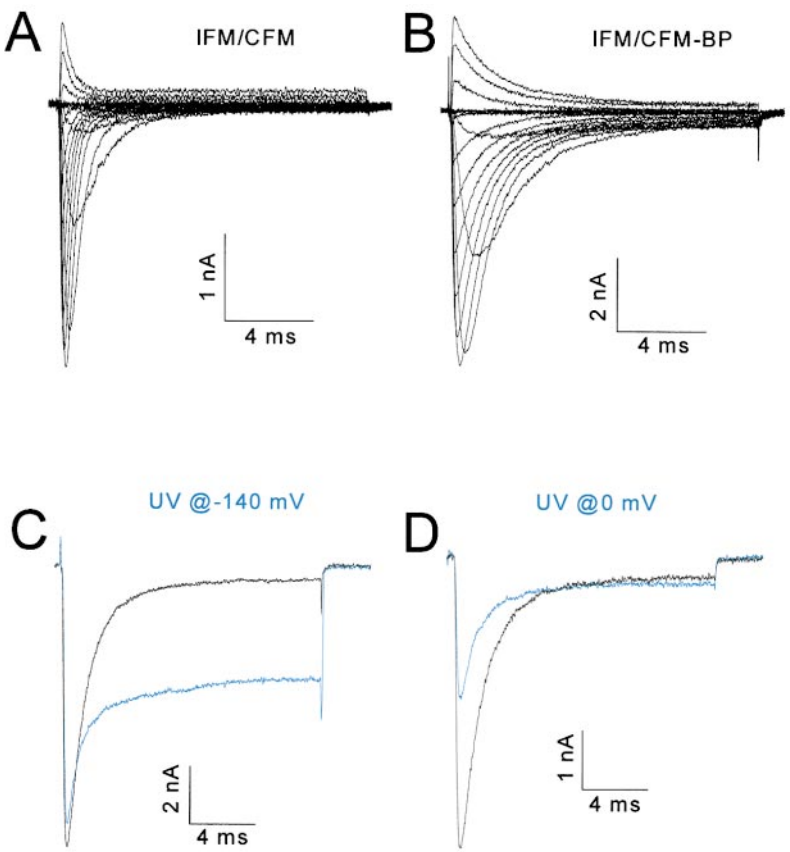


Figure 2. Immobilizing the inactivation gate. All data from the IFM/CFM mutant of the human skeletal muscle sodium channel. Blue traces show currents after exposure to UV light. (A and B) Families of currents in response to depolarizations from −90 to +60 mV in 10-mV increments from a holding potential of −140 mV. The cell in A is unlabeled and in B is labeled with BPMTS (62.5 mM placed into the pipette solution). The inactivation time constants were well fit by single exponentials in both cases, and by a mixture of these two exponentials only during the modification by BPMTS (data not shown), strongly suggesting that all cysteines were labeled with benzophenone at the time of UV irradiation. All recordings obtained >10 min after achieving the whole cell configuration. (C) Currents at −20 mV for a BPMTS-labeled cell before and after exposure to 26 s of filtered UV light presented at the −140-mV holding potential. (D) Currents at −20 mV for another labeled cell before and after exposure to UV light delivered during six 2-s depolarizations to 0 mV. Each 2-s depolarization was followed by a 6.5-s hyperpolarization to −150 mV to recover (>95%) from slow inactivation. The time constant of inactivation at −20 mV in nine BP-labeled cells ranged between 1.27 and 1.52 ms and was not affected statistically by UV irradiation (*t* test, $P > 0.1$). The total exposure time at depolarized and hyperpolarized voltages differed only because we stopped the experiment when UV had no further effects.

twofold. First, gating currents, which are believed to be caused primarily by the movement of charged S4 residues, are easily resolved in whole-cell recording of *Shaker* due to the high expression levels (Melishchuk et al., 1998). Second, because each channel has four identical S4 segments, we can make quantitative predictions for the relative effects of S4 immobilization on gating and ionic currents.

The mutation A359C was introduced into a *Shaker*-IR construct that has no N-type inactivation and marginal C-type inactivation (Melishchuk et al., 1998). The introduced cysteine at the extracellular end of the S4 segment was chosen because this residue is known to change its local environment when the channel is depolarized, and because labeling here with large fluorophores has little effect on gating current (Mannuzzu et al., 1996; Cha and Bezanilla, 1997, 1998). The A359C mutant functioned robustly when labeled with BPMTS (A359C-BP; Fig. 3 A) and was therefore optimal for our study.

We expected that immobilizing a single S4 segment at a hyperpolarized voltage, when it should be in its "resting" or "inward" conformation, would have two consequences on channel function. It should only partially reduce an individual channel's gating current if other S4 segments remain capable of moving, and it should prevent the channel from opening. The latter consequence follows from the assumption that all four S4 segments must be able to translocate their charges outward for the channel to be able to open. Therefore, irradiation of BP-labeled *Shaker* S4 segments is expected to reduce the ionic current proportionally more than the gating current. Quantitatively, we can predict the relationship between peak gating current and ionic current as follows.

We assume that all S4 segments are labeled by BPMTS, based on the fact that a 200-fold lower concentration of a less-reactive reagent, tetramethylrhodamine maleimide, completely labels residue A359C of *Shaker*[2] (Mannuzzu et al., 1996). We also assume, without direct evidence, that all of the labeled residues have a functional benzophenone moiety. Let $p_{S4}(t)$ be the probability that an S4 segment has not been immobilized at time $t$ during irradiation, and $p_{Ch}(t)$ be the probability that the channel is functional. Because of tetrameric stoichiometry:

$$p_{Ch}(t) = p_{S4}^4(t). \quad (1)$$

When exposed to UV light for a period of time, $t$, any of three outcomes is possible for each benzophenone. It may have inserted (cross-linked) into a neighboring region of protein, it may remain unchanged, or its ability to immobilize the S4 segment may have been destroyed by the UV light.[3] Only if the benzophenone is unchanged does it have the possibility of inserting when exposed again to UV. We denote the rate of cross-linking as $\alpha$ and the rate of destruction as $\beta$, as shown in Scheme I.

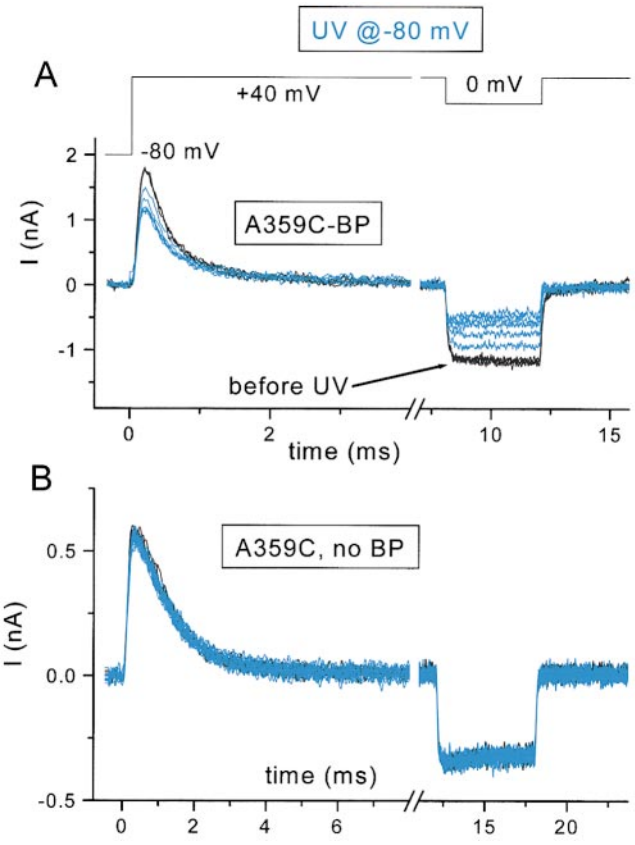


Figure 3. Effect of UV irradiation on the A359C mutant of *Shaker*-IR. UV applied at the −80-mV holding potential. Outward gating currents at +40 mV and inward ionic currents at 0 mV are shown. Control traces in black and after UV in blue. (A) Effect of UV (six 4-s exposures) after three control depolarizations. (B) Effect of UV on an unlabeled cell (three control and 20 UV traces, each with 4-s exposure).

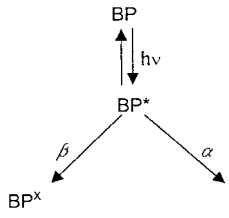


(SCHEME I)

[2]We exposed our cells to 1 mM BPMTS for 10 min at room temperature. Mannuzzu et al. (1996) used 5 μM tetramethylrhodamine maleimide on ice for 30 min.

[3]Photodestruction of benzophenone could be caused by, among other possibilities, the oxidation of either the alkyl or ketyl radicals that are generated by the H-atom abstraction in the first step of cross-linking (Dormán and Prestwich, 1994). Benzophenone might also insert into a location that doesn't immobilize the S4 segment.

Where BP represents functional benzophenone in the ground state, BP* represents benzophenone in a triplet excited state, $BP^{\times}$ is benzophenone after photodestruction, and BP-Protein represents a cross-linked benzophenone. The effect of UV irradiation is expected to be first order. Therefore:

$$p_{S4}(t) = (1 - w) + we^{-\lambda(\alpha+\beta)t}$$
$$w = \alpha/(\alpha + \beta). \quad (2)$$

The relative probability of the benzophenone being in the excited rather than ground state is λ. Note that if the rate of photodestruction of benzophenone is negligible (i.e., $\alpha >> \beta$), then $p_{Ch}(t)$ will be exponential with a rate four times greater than that of $p_{S4}(t)$. However, $\alpha < \beta$ in our experiments (see below). Therefore, the decay of $p_{Ch}(t)$ is expected to be multi-exponential and more comparable in overall rate with that of $p_{S4}(t)$. We estimate $p_{Ch}(t)$ from the decrease in amplitude of ionic current as a function of exposure to UV light in BP-labeled channels. The effect of UV on gating currents depends on the possible cooperative interaction among S4 segments (see below and appendix).

To measure gating current and ionic current in the same experiment, we used low concentrations of a poorly permeant cation, cesium, and depolarized a cell first to the reversal potential of the ionic current (approximately +40 mV in our experiments) to record the gating current, and then to either 0 or +70 mV to record ionic current through open channels. Under these conditions, the ionic and gating currents are comparable in magnitude (Fig. 3 A). The initial depolarization used to activate the gating current is sufficiently positive to maximally open these channels. Moreover, the conductance–voltage curve reaches a plateau by 0 mV (Fig. 4), minimizing the contamination of the ionic currents in Fig. 3 by gating currents.

UV irradiation of A359C-BP at a hyperpolarized voltage reduced both ionic and gating currents (Fig. 3 A), and, as predicted above, the inward ionic current at 0 mV was reduced more than the gating current. Comparable exposure of unlabeled A359C channels to UV light had no effect (Fig. 3 B). The relative time courses of current reduction for normalized data are plotted in Fig. 5 for five cells. For these experiments, we measured the ionic current at +70 mV, avoiding any possibility of reducing the open probability by a step from +40 to 0 mV. The reduction of ionic current (Fig.5, ▼) was fit by a single exponential function raised to a fourth power (Eqs. 1 and 2) with a time constant of 6.0 ± 0.8 (units of number of UV flashes). Only ~27% of the S4 segments are immobilized at steady state ($w = 0.267 \pm 0.018$), indicating that $\beta \simeq 2.7\ \alpha$. In other words, photoexcitation of the benzophenone is nearly three times more likely to destroy its function than to result in an immobilizing insertion.

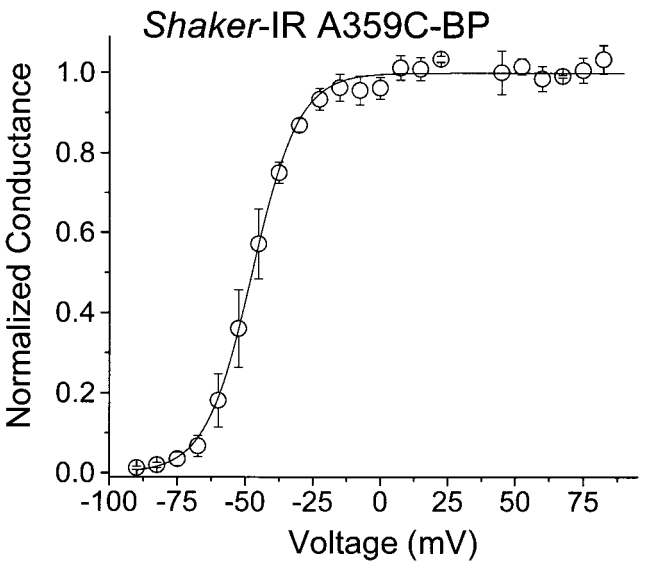


Figure 4. G-V relationship measured at the end of a 20-ms depolarization for *Shaker*-IR A359C-BP. The Boltzmann curve has a midpoint of −47.4 ± 2.9 mV and a slope of 2.9 ± 0.4 $e_0$ ($n$ = 3 cells).

If S4 segments are completely independent in their movement (i.e., immobilization of an S4 segment has no effect on the movement of other S4 segments), then the reduction of gating current is predicted by the fourth root of the reduction of ionic current. Fig. 5 shows that this prediction holds reasonably well (○ and solid line). Alternatively, a fraction of gating charge movement, $f_{coop}$, may be cooperative. We estimated $f_{coop}$ from the data in Fig. 5 (see appendix for details). The moderately improved fit (Fig. 5, dotted line) is associated with an estimate for $f_{coop}$ of 0.045 ± 0.026, a value bordering on statistically different from zero ($P \cong 0.05$). However, a likelihood ratio test shows no improvement in fit for a model including cooperativity ($P > 0.05$). Our data are also inconsistent with a model in which cross-linking reduces only part of the charge movement of a single subunit. In this case, the reduction of gating current would be less than observed for the above model.

These results suggest that photocross-linking of a single S4 segment (a) immobilizes the bulk of its charge movement, (b) prevents channel opening, and (c) has little effect on gating current generated by the remaining S4 segments of a channel. Taken together, the data show that an S4 segment can be immobilized at a hyperpolarized voltage.

*State Dependence of S4 Immobilization in Shaker*

S4 segments are believed to have at least two conformations, representing the limits of their positions with respect to the membrane electric field. At the hyperpolarized voltage we examined in the above experiments,

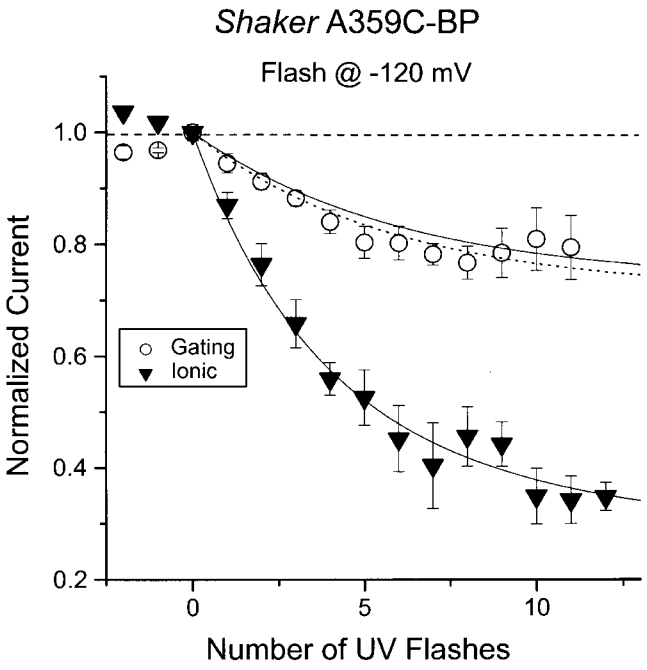


Figure 5. Relative reduction of peak gating current and ionic current for *Shaker*-IR A359C-BP Same as for Fig. 3, except using flash-lamp stimulation and measuring the ionic current at +70 mV. Solid curves are the best fit to an independent model (see appendix). The dashed line shows the predicted gating current reduction for a model including cooperativity ($f_{coop}$ = 0.045). Data for $n$ = 5 cells are shown.

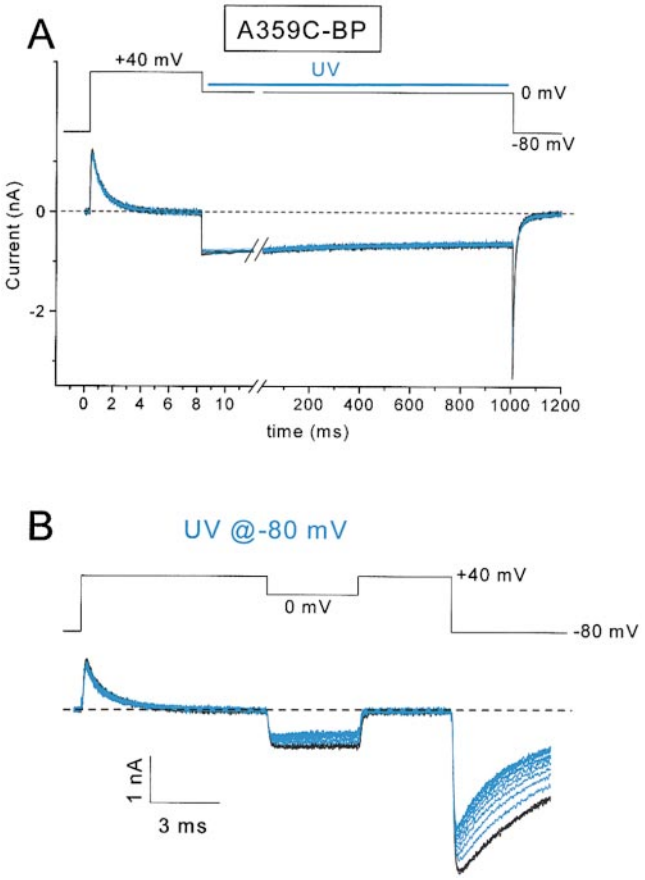


Figure 6. State-dependent photocross-linking of *Shaker*-IR A359C-BP. (A) 3 control (black) and 10 experimental traces (blue) using 1-s exposures of UV. Little current reduction was observed. The UV was applied 20 ms after the step to 0 mV and was terminated 20 ms before the return to the holding potential. (B) 3 control and 13 UV-irradiated traces for a subsequent treatment of the same cell in A, except that UV was applied at the −80-mV holding potential.

the S4 positive charges tend to be in an inward position with respect to the field and, at voltages more positive than 0 mV, they tend to be in an outward conformation. We therefore tested whether S4 segments could be immobilized in an outward conformation by irradiating BP-labeled channels at 0 mV. If so, one possible result would be a greater ease in opening the channel by depolarization, because fewer S4 segments would have to move to achieve this end. However, Fig. 6 A shows that UV light presented during ten 1-s exposures at 0 mV[4] had little effect on either gating currents at +40 mV or inward ionic currents at 0 mV. UV irradiation caused a small (4.4%) reduction of ionic current in this cell, and a somewhat larger (13%) reduction in another cell under identical conditions.

The result in Fig. 6 A has three possible explanations: (a) the S4 segments were either inadequately labeled or inadequately exposed to UV light, (b) the benzophenones inserted into a region of the protein that was incapable of immobilizing the S4 segment, or (c) the depolarization moved the benzophenone labels into a position where they were less capable of reaching a suitable target for insertion. To discriminate these possibilities, we next irradiated the same cell under the same conditions, except at a −80-mV holding potential (Fig. 6 B). Three control traces (black) are superimposed before presenting 13 exposures to UV light (4 s each). This treatment caused a net decrease in both the gating current (12.7% reduction) and the ionic current at 0 mV (47.7% reduction).[5] The reduction in ionic current is reasonably close to the predicted 42%, based on the independence assumptions used in Eq. 1. The relatively modest reductions observed for this cell (Fig. 6 B), compared with data shown in Figs. 3 and 5, is likely the result of the photodestruction of a fraction of the benzophenone labels during the UV exposure at 0 mV for the experiment of Fig. 6 A.

[4]The slow decrease in ionic current during the 1-s depolarizations (note the change in the time base) is likely to be due to a residual C-type inactivation in this mutant.

[5]The tail currents at −80 mV in Fig. 6 are a mixture of gating and ionic currents. Therefore, we did not use their amplitudes to assess the effects of UV irradiation.

These data show a state dependence for the cross-linking of the *Shaker* S4 segment labeled at residue 359. The immobilization is more efficient at hyperpolarized voltages, apparently because depolarization moves the benzophenone to a position where it is less capable of inserting into a neighboring region of protein. In another series of experiments, using different ionic conditions, we found that S4 segments were immobilized 2.3× faster for UV flashes at −120 than at 0 mV (data not shown).

The above experiments with the inactivation gate and with *Shaker* S4 segments show that moving parts can be immobilized. Immobilization depends on the state of the moving part (gate: closed or open; voltage sensor: extended or retracted). In both cases, irradiation apparently produces a complete effect in that cross-linking does not partially impede or slow movement; it completely immobilizes the gate or S4 segment. There are no changes in the kinetics of either inactivation or gating current. Furthermore, the effects appear to be local, in that other mobile parts of the channel remain functional.

*Immobilization of S4 Segments in Sodium Channels*

Given that S4 segments in *Shaker* potassium channels can be immobilized by photocross-linking, we examined the consequences of immobilizing either of two sodium channel voltage sensors, the S4 segment in domain 2 (D2/S4) or the S4 segment of domain 4 (D4/S4). D2/S4 is believed to be coupled primarily to the activation gate (Chen et al., 1996; Kontis and Goldin, 1997; Kontis et al., 1997; Mitrovic et al., 1998; Cha et al., 1999a), whereas D4/S4 is believed to be the main voltage sensor coupled to inactivation (Chahine et al., 1994; Chen et al., 1996; Kontis and Goldin, 1997; Kontis et al., 1997; Cha et al., 1999a). To test for state dependence, we examined the effect of irradiating labeled S4 mutants at either hyperpolarized voltages or depolarized voltages.

In D2/S4, we used the cysteine mutant of the outermost basic residue (D2:R1C; Mitrovic et al., 1998). Fig. 7 A shows the current for D2:R1C-BP at a test voltage of −20 mV, before (black) and during (blue) UV irradiation. In this experiment, UV was flashed at the −140-mV holding potential. The current after each flash, applied every 10 s, is shown. The reduction of current was uniform over all voltages (Fig. 7, B and C), suggesting that immobilization of this voltage sensor destroys channel function, presumably by preventing activation gates from opening. The time course of current reduction was similar when the xenon lamp was flashed either at +20 mV or at the holding potential (Fig. 7 D). In control experiments with unlabeled cells, irradiation under identical conditions did not reduce the amplitude of the peak current (Fig. 7 D, ◇).

These data support a role for D2/S4 in the process of activation. Immobilization of D2/S4 at either hyperpolarized or depolarized voltages prevents channels from opening.

By contrast to D2/S4, the D4/S4 segment plays a predominant role in the kinetics and voltage dependence of fast inactivation (Chahine et al., 1994; Chen et al., 1996; Kontis and Goldin, 1997; Cha et al., 1999a; Sheets et al., 1999). We examined three cysteine mutants in this transmembrane segment: D4:R1C, D4:R3C, and D4:R4C, corresponding to the first (outermost), third, and fourth basic residues. D4:R1C and D4:R4C are accessible to hydrophilic cysteine reagents only from the extracellular or intracellular sides, respectively, of the channels, whereas D4:R3C is translocated by depolarization from an intracellular to an extracellular position (Yang et al., 1996).

Fig. 8, A and B, shows that UV irradiation of extracellularly labeled D4/S4 mutants has a qualitatively different effect from that observed for *Shaker* and for the D2/S4 mutant. Instead of decreasing the peak current while having only minor effects on kinetics, irradiation of either D4:R1C-$BP_{out}$ or externally labeled D4:R3C (D4:R3C-$BP_{out}$) causes an increase in current amplitude and a marked slowing of inactivation kinetics. Similar effects were seen whether the cells were irradiated at hyperpolarized or depolarized voltages (data not shown). These results show that immobilizing D4/S4 decreases the effectiveness of inactivation. The increase in peak current could be due to a decrease in the rate of inactivation of both closed and open channels after a depolarization (Gonoi and Hille, 1987).

These effects of irradiation, increase of current amplitude, and slowing of inactivation are only observed when the D4/S4 cysteines are labeled extracellularly. Fig. 8, C and D, shows that irradiation of D4:R3C and D4:R4C at a hyperpolarized voltage, after intracellular labeling, causes a reduction of current with less effect on the kinetics of the currents, reminiscent of the consequence of immobilizing the D2/S4 segment (Fig. 7). Although the reduction of current for D4:R3C-$BP_{in}$ is small (18.7 ± 2.4%, $n = 7$), it was a rapid and saturable effect of UV that was observed in all cells. Furthermore, unlabeled D4:R3C showed little current reduction in response to a comparable exposure to UV (3.4 ± 0.9% reduction, $n = 5$).

The contrast between irradiating extracellularly and intracellularly labeled D4:R3C is striking and suggests the possibility that the channels function differently depending on the side of the membrane on which the BP-MTS was applied to the channels. However, the biophysical consequences of labeling are rather comparable for these two labeling conditions (Fig. 9, Table I). The only significant difference is a less than twofold increase in the inactivation time constant for intracellular

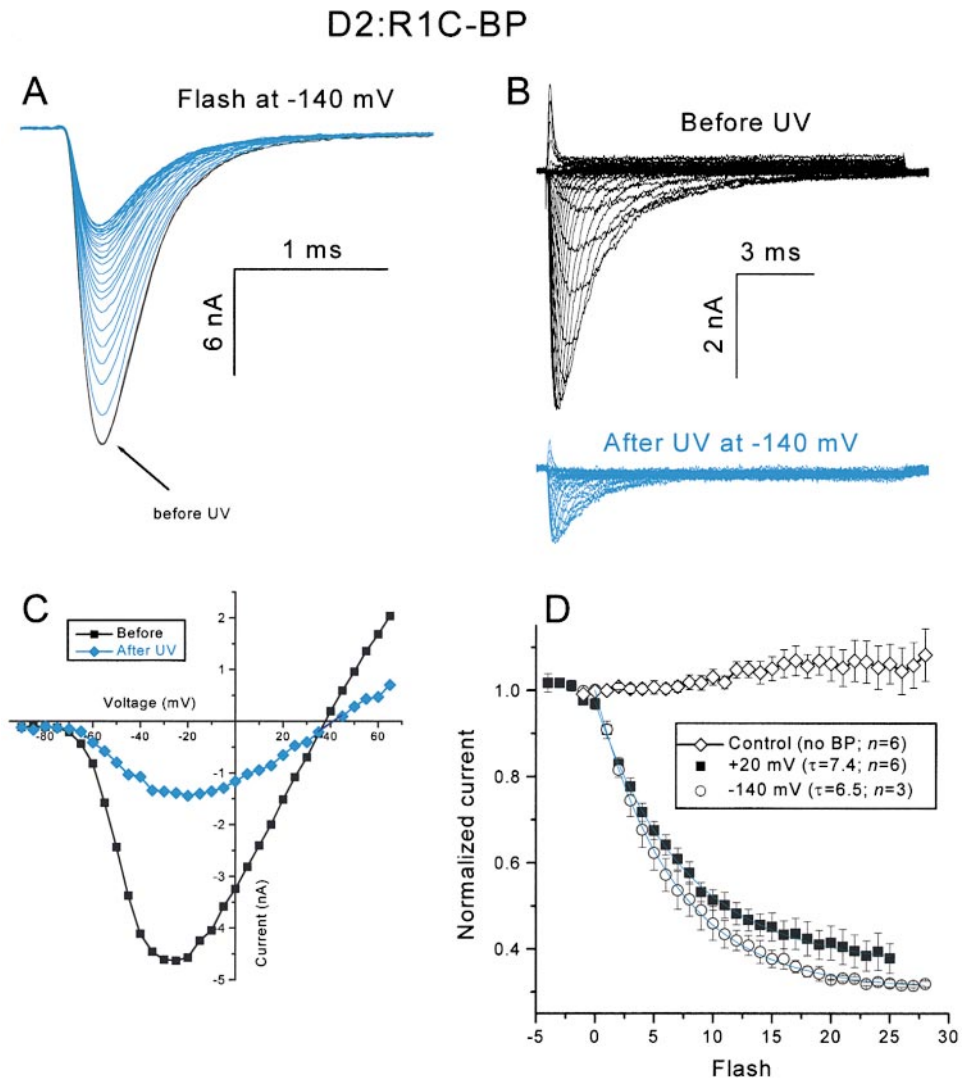


Figure 7. Immobilization of D2/S4. All experiments were done with the D2:R1C mutant, and all UV irradiation used a flash lamp. Labeling was done by exposing cells in a tissue culture dish to 1 mM BPMTS for 10 min. The labeling caused a small increase in the inactivation time constant at depolarized voltages and an ~15-mV depolarizing shift of the G-V curve (see Mitrovic et al., 1998). (A) Currents at −20 mV before (black) and after (blue) exposure to UV flashes. Successive flashes were applied at the −140-mV holding potential every 10 s. (B) Families of currents (−90 to +60 mV in 10-mV increments from a −140 mV holding potential) from another cell before and after exposure to UV flashes. The peak I-V relationship for this cell is shown in C. (D) Normalized peak current at −20 mV for cells flashed either at the −140-mV holding potential (○) or at +20 mV (■). (◇) Effects of irradiation at the holding potential on unlabeled D2:R1C cells.

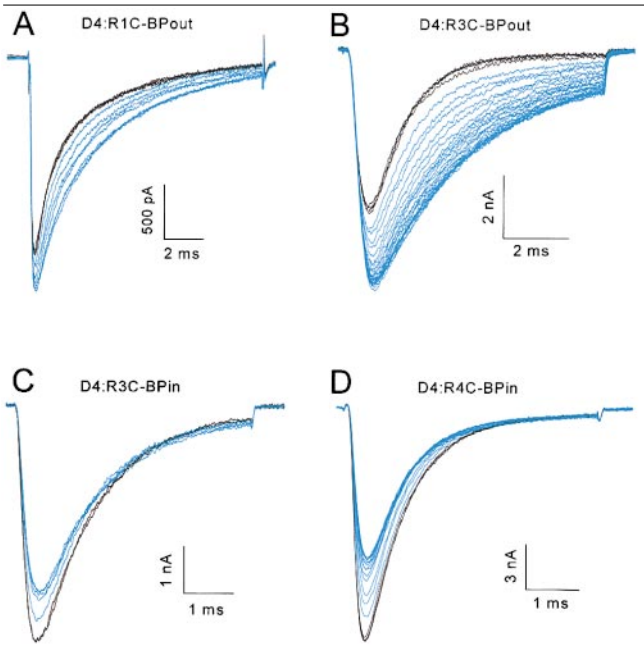


Figure 8. Photocross-linking D4/S4 mutants. Black and blue traces represent currents before and after, respectively, exposure to continuous-power UV light at the holding potential of −150 mV. All cysteine mutants were labeled with BPMTS. (A) D4:R1C-BP currents at 0 mV. Traces show progressive effects of 4.2-s exposures to UV light. This residue was labeled externally. (B) D4:R3C labeled with extracellular BPMTS. Currents at −30 mV using 4-s exposures to UV light. (C) D4:R3C labeled with intracellular BPMTS (125 μM in the pipette solution). Currents at −30 mV using 4-s exposures to UV light. (D) D4:R4C labeled with intracellular BPMTS (125 μM in the pipette solution). Currents at −45 mV using 4-s exposures to UV light. The current reductions seen in C and D were uniform over all voltages, as seen for D2:R1C-BP in Fig. 7 C.

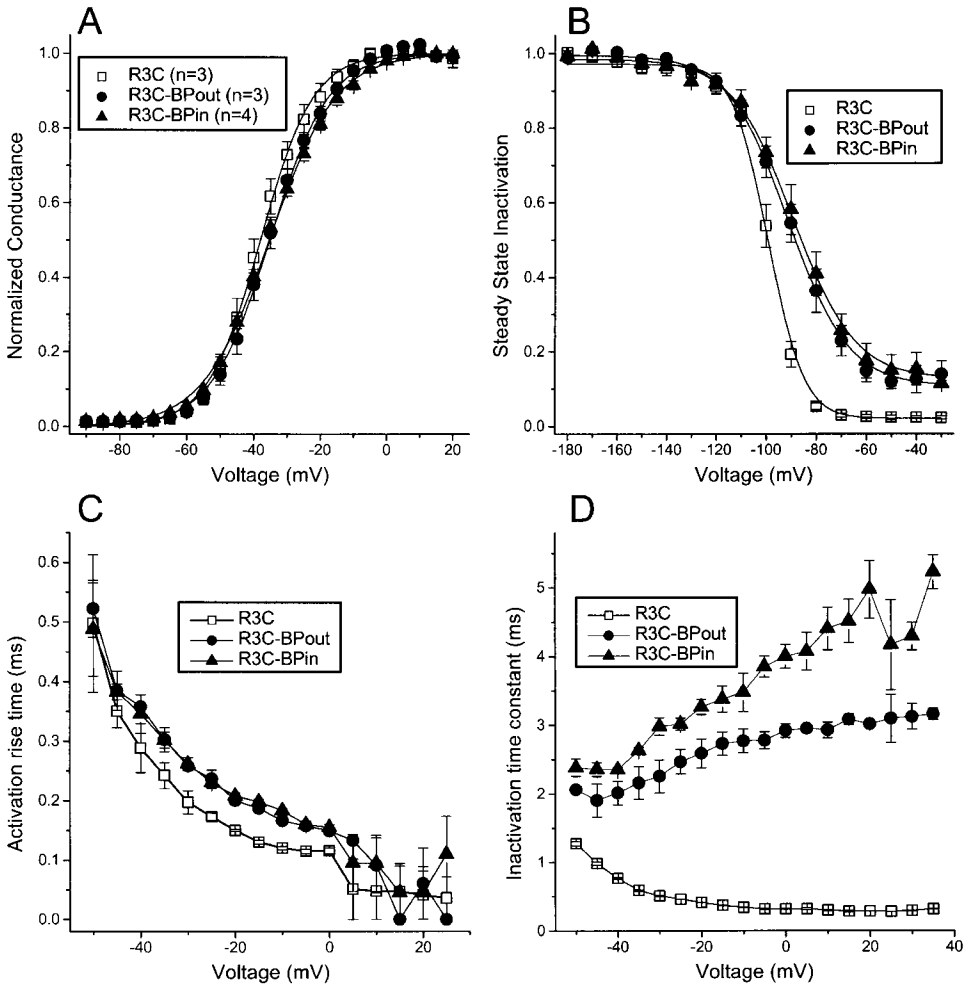


Figure 9. Biophysical effects of modifying D4:R3C with BPMTS in the absence of UV irradiation. (A) Normalized peak conductance–voltage relationship for R3C, either unmodified, modified with extracellular BPMTS (R3C-BPout), or modified with intracellular BPMTS (R3C-BPin). Parameters ($V_{mid}$, $q$) for Boltzmann fits are in Table I. (B) $h_\infty$ curves using 100-ms prepulses to the indicated voltage. Parameters ($V_{mid}$, $q$) for Boltzmann fits are in Table I. (C) 10–90% rise time for activation. (D) Inactivation time constants from single exponential fits to the current decay after a depolarization.

versus extracellular labeling (Fig. 9 D). The dramatic difference in response to UV irradiation suggests, however, that the benzophenone adduct attached to the cysteine thiol of D4:R3C remains restricted to the side of the channel to which it was applied. In other words, within the limits of our experiments, S4 movement is incapable of translocating the benzophenone adduct through the gating pore. If the adduct could distribute itself readily across the channel protein, the biophysical consequences of labeling and the response to UV irradiation would be more similar, wherever the label was originally attached to this residue. This conclusion contrasts with previously published data showing that a smaller cationic adduct, ethyltrimethyammonium, can be translocated by D4:R3C (Yang et al., 1996).

TABLE I

*Biophysical Parameters of D4:R3C Current, either Unmodified, Internally Modified, or Externally Modified by BPMTS*

| | Control | Internal | External |
|---|---|---|---|
| | *n = 3* | *n = 3* | *n = 3* |
| G-V, $V_{mid}$ (mV) | −38.0 ± 1.8 | −35.3 ± 0.68 | −35.2 ± 1.5 |
| $q$ ($e_o$) | 3.33 ± 0.16 | 2.62 ± 0.12 | 2.98 ± 0.09 |
| $h_\infty$, $V_{mid}$ (mV) | −99.1 ± 1.3 | −89.1 ± 2.5 | −91.1 ± 3.4 |
| $q$ ($e_o$) | 4.22 ± 0.04 | 2.20 ± 0.16 | 2.23 ± 0.07 |

Data obtained from parameters (midpoint and slope) for Boltzmann fits to the G-V and $h_\infty$ curves in Fig. 9, A and B.

Our experiments support the idea that individual S4 segments of the sodium channel play different roles in gating, with D2/S4 acting primarily as a voltage sensor for activation. Immobilization of D4/S4 has effects both on the opening of the activation gate and on the closing of the fast inactivation gate, suggesting that it serves as a voltage sensor for both activation and inactivation.

## DISCUSSION

With the exception of some structural molecules, proteins are designed to move. The range of protein motion is extensive, from shear motions of ~1 Å in an aspartate receptor (Ottemann et al., 1999) to the dramatic movements of motor proteins (Vale and Milligan, 2000) and of at least one type of ion channel (Slatin et al., 1994). Protein movements have been characterized using a diversity of approaches that include structural

snapshots (Subbiah, 1996) and dynamic measurements that encompass both electrophysiological and spectroscopic (e.g., Weiss, 1999; Forkey et al., 2000; Hubbell et al., 2000) techniques. The goal of our study was not to measure protein movements of ion channels, but to examine the consequences of preventing the movement of specific regions of the channels. The long-term goal is to try to understand how movements within voltage-gated channels are coupled.

We combined cysteine mutagenesis with a newly designed bifunctional reagent, BPMTS, which has a photoactivatable cross-linking moiety. This approach has the potential of allowing us to cross-link an introduced cysteine with a neighboring region of the ion channel without knowing a priori the identity of the residues close to the cysteine. We introduced cysteines into the two regions of ion channels believed to undergo significant movement, gates and voltage sensors (Yellen, 1998), and our results suggest that both can be immobilized selectively. First, the fast inactivation gate of the sodium channel, labeled with BPMTS, can be immobilized in either its open or its closed conformation by irradiating the channel at a hyperpolarized or a depolarized voltage, respectively (Fig. 2). Second, immobilization of an S4 segment of *Shaker* potassium channels reduces both gating and ionic current (Fig. 3), with relative magnitudes of reduction predicted by the homotetrameric stoichiometry of these channels (Fig. 5).

Because of the length of the linker between the introduced cysteine and insertion site ($\sim$10 Å), and the reaction radius around the ketone oxygen of benzophenone ($\sim$3 Å; Dormán and Prestwich, 1994), this experimental approach is likely to be limited to the study of movements of at least several angstroms between either two domains or two secondary structural elements. The fact that we were able to immobilize both the inactivation gate of the sodium channel and the S4 segments of potassium channels suggests that movements of both structures satisfy this limitation.

The magnitude of gate movement in voltage-gated ion channels is unknown. However, the gate movements of a bacterial potassium channel have been studied using site-directed spin-labeling methods (Perozo et al., 1999). For this channel, gate opening was accompanied by an $\sim$20° rotation of a transmembrane $\alpha$ helix, which corresponds to a sidechain movement of $\sim$2 Å. Two recent studies of S4 movement, using spectroscopic measurements based on resonance energy transfer, suggest motion in the range of 1–10 Å between voltage sensors in different subunits (Glauner et al., 1999; Cha et al., 1999b). Estimates of S4 movement based on its electrostatic interactions with a charged pore blocker fall into a similar range (3–8.5 Å; French et al., 1996). However, the magnitude of the relative movement between an S4 segment and the protein immediately surrounding it is unknown. Nevertheless, our experiments indicate that both gate movement and voltage-sensor movement are sufficiently large that photocross-linking can immobilize either one using BPMTS.

*Comparison with Other Methods of Protein Immobilization*

Although photocross-linking allows a systematic approach to immobilizing specific regions of ion channels, other strategies have been explored. Many are based on the binding of a molecule to a mobile region. For example, binding of certain peptide toxins to the S3–S4 loops of voltage-gated ion channels may partially inhibit voltage sensor movement (Sheets and Hanck, 1995; Swartz and MacKinnon, 1997a,b; Cestèle et al., 1998). Also, antibodies directed against the inactivation gate of the sodium channel partly hinder its ability to close (Vassilev et al., 1988).

A dramatic effect of streptavidin binding to a mobile biotinylated region of the Colicin Ia toxin ion channel (Slatin et al., 1994) led us to try this approach also. We biotinylated cysteines introduced into S4 segments, but the binding of streptavidin had little effect on gating (data not shown). We tentatively concluded that the S4 movements were too small to be perturbed by the streptavidin, perhaps because the linker between the cysteine and biotin was too long or too flexible.

A particularly powerful, and widely exploited, method of gate immobilization is the use of reversible open-channel blockers that prevent gate closure by a "foot-in-the-door" mechanism (Armstrong, 1971; reviewed in Yellen, 1998). In its purest form, pore occupancy by a blocker and gate closure are mutually exclusive, and the rate of gate closure can be predicted simply from the concentration and affinity of the blocker.

Several methods of immobilization are based on the introduction of cysteines into the channel protein. Oxidation of cysteines, for example, with methanethiosulfonate reagents, may inhibit gate closure if these residues are located near critical gating machinery (Yellen, 1998). Furthermore, the tight binding between a cadmium ion and either two cysteines (Liu et al., 1997), or a cysteine and a histidine (Holmgren et al., 1998), can trap the conformation of the activation gate. Finally, disulfide trapping may be employed to form a covalent link between two regions of an ion channel, if the introduced cysteines come into close enough proximity (e.g., Zhan et al., 1994; Liu et al., 1996; Bénitah et al., 1997; Tsushima et al., 1997). Although these methods allow a systematic exploration of a region of interest, they have drawbacks. Whereas oxidation of S4 cysteines, for example, with methanethiosulfonate reagents, can affect gating, this may not be a consequence of a restriction of motion. It may instead be one of a myriad of allosteric effects due entirely to changes in the structure of the sidechain at that position. Cadmium and disul-

fide trapping have the potential of immobilizing the relative movements of two protein regions. However, it is often a matter of luck to find residues that are close enough to be able to create a metal binding site or form a disulfide bond between them, without prior knowledge of a high-resolution structure. Our approach requires the use of only a single cysteine, which can be introduced wherever it seems appropriate.

One of the principal drawbacks of photocross-linking with BPMTS is that the efficiency is always <100%, leaving a fraction of channels that have benzophenone-labeled cysteines, but are not cross-linked. This produces a heterogeneous population of channels with heterogeneous biophysical properties. Nevertheless, our experiments generated several insights about both gates and voltage sensors.

*Fast Inactivation*

The fast-inactivation gate of the sodium channel was long believed to be a tethered intracellular blocker of open channels (Armstrong and Bezanilla, 1977; Bezanilla and Armstrong, 1977). More recent studies using mutagenesis and cysteine scanning suggest that the cytoplasmic linker between D3 and D4 of the sodium channel is the tethered inactivation gate (West et al., 1992; Patton et al., 1992; Kellenberger et al., 1996). The most important part of this postulated gate is a cluster of three consecutive residues (IFM) in the D3-D4 linker, with the central phenylalanine acting as a crucial player in effective closure of the gate. For this reason, we initially examined the cysteine mutant of this residue (IFM/ICM). However, labeling of this mutant with BPMTS alone almost completely abolished inactivation (data not shown), so that it was difficult to study the state-dependent effects of cross-linking it by UV irradiation. Therefore, we switched to the cysteine mutant of isoleucine (IFM/CFM). Labeling of this residue also inhibits inactivation, but the effect is more moderate (Fig. 2, A and B). Irradiation after labeling allowed a selective immobilization of the inactivation gate (Fig. 2, C and D), supporting the hypothesis that the D3–D4 linker is the fast-inactivation gate.

Our results with the IFM/CFM mutant may be examined in context of the nuclear magnetic resonance solution structure of the isolated D3–D4 linker (Rohl et al., 1999). The structure shows that the adjacent residues isoleucine and phenylalanine are both on a solvent-exposed surface, and therefore potentially available to interact jointly with a binding site for the inactivation gate (Rohl et al., 1999). This is consistent with the fact that the cysteine of the IFM/ICM mutant is accessible to hydrophilic reagents only when the inactivation gate is open (Kellenberger et al., 1996). Our results further suggest that the open inactivation gate is in the vicinity of a region other than the binding site that normally closes the gate, because irradiation of open inactivation gates prevents them from closing.

*Immobilization of Shaker's S4 Segment*

The relative reduction of gating and ionic current, due to photocross-linking *Shaker* S4 segments, approximately follows a fourth power relationship (Eq. 1, Fig. 5). This result is in accordance with three assumptions: (a) cross-linking completely prevents charge movement of an individual S4 segment, (b) immobilizing a single S4 segment prevents channel opening, and (c) S4 segments move independently.

In our experiments, only ~27% of the gating current was abolished by irradiation (Fig. 5). This agrees with other experimental results using benzophenone-based cross-linking reagents. The maximal labeling efficiency of benzophenone is highly variable, and rarely surpasses 70% (Dormán and Prestwich, 1994). However, if the immobilization of individual S4 segments is random, and therefore follows binomial statistics, a 27% level of immobilization indicates that ~30% of the channels have more than one immobilized S4 segment. This is a high enough efficiency to lend support to our conclusions about the independence of S4 segments, which in this context means that if an S4 segment of a *Shaker* potassium channel is immobilized, the other S4 segments in the channel are oblivious to this event. We can say, with even more confidence, that immobilization of a single S4 segment does not completely prevent the other S4 segments from moving. If this were the case, the fractional reduction of ionic and gating current would superimpose. The reasonable agreement of our results with the above three assumptions suggests, therefore, that cross-linking has the desirable, and perhaps surprising, consequence of producing a local, rather than global, effect on the protein, a conclusion consistent with our experiments with labeled inactivation gates.

Our evidence for a predominantly independent movement of S4 segments supports previous results on *Shaker*, based on the biophysical consequences of mutagenesis of the S4 segment (Tytgat and Hess, 1992; Bezanilla et al., 1994; Schoppa and Sigworth, 1998; Smith-Maxwell et al., 1998a,b; Ledwell and Aldrich, 1999; however, see Mannuzzu and Isacoff, 2000). These studies suggest that the bulk of gating charge movement corresponds to the independent movements of individual S4 segments. Only the final conformational changes along the activation pathway (i.e., near the open state) involve a cooperative movement of all the S4 segments. These final transitions, which involve movement of other structures besides the S4 segments, carry only a small fraction of the total gating charge.

Like cross-linking of the inactivation gate, the immobilization of the *Shaker* S4 segment is state dependent,

occurring more readily at hyperpolarized voltages when S4 is situated in an inward conformation with respect to the electric field. At a depolarized voltage, the S4 segment, labeled at residue 359, inserts less readily into a neighboring region (Fig. 6). This result agrees well with voltage-dependent fluorescence measurements obtained from *Shaker* A359C labeled with tetramethylrhodamine. Depolarization reduces the anisotropy of the fluorophore and increases its accessibility to collisional quenchers, as if depolarization moves it out of a constrained environment (Cha and Bezanilla, 1998). In a similar manner, A359C-BP can find an insertion target most easily in its constrained environment at a hyperpolarized voltage.

Our results with *Shaker* show that an S4 segment can be immobilized in a state-dependent manner, but this result may depend on the specific residue that is labeled and how its environment changes with changes in membrane potential. This proviso especially applies to sodium channels, where the primary sequence of amino acids in each domain is different.

*Immobilization of S4 Segments of Sodium Channels*

Irradiation of the S4 segment of domain 2, using D2:R1C-BP, prevented the channels from functioning. This suggests that, as in *Shaker*, the ability of D2/S4 to move with respect to its surrounding "gating pore" (the hydrophobic region that encircles the S4 segment) is essential for a channel to open.

There are, however, some distinctions between D2/S4 and *Shaker* S4. First, the efficiency of cross-linking is $\sim$2.7$\times$ higher in D2/S4 because, although the magnitude of reduction of ionic current ($\sim$70%) is similar (Figs. 5 and 7), *Shaker* has four labeled S4 segments. The higher efficiency in D2/S4 may be a consequence of the fact that the benzophenone is more appropriately situated with respect to an insertion site, perhaps because the outer vestibule surrounding the S4 segment is narrower in sodium channels. Another difference between *Shaker* S4 and D2/S4 is that immobilization of D2/S4 is nearly independent of membrane potential (Fig. 7 D). This implies that D2/S4 must be capable of moving for the channel to function, and that even if it is immobilized in its outward conformation with respect to the electric field, the activation gates cannot open. By contrast, the *Shaker* S4 segment, labeled at residue 359, is harder to immobilize when in an outward conformation. This contrast also suggests a different local environment near the extracellular ends of the S4 segments of *Shaker* and sodium channels.

The absence of a strong state dependence of S4 immobilization was a consistent feature of several sodium channel mutants we examined, regardless of the specific biophysical consequences of photocross-linking. This suggests that immobilization per se is sufficient to alter function, regardless of the S4 segment's conformation when it was immobilized. This result further implies that some voltage-dependent movement must occur in the immediate vicinity of the benzophenone moiety. If no movement occurred, it is hard to imagine how the photocross-linking could so profoundly disrupt function.

The two distinguishing features of immobilization of sodium channel S4 segments are the domain of S4 origin and where (intracellular or extracellular) the BP-MTS was applied to an S4 segment. As in *Shaker*, immobilization of D2/S4 appears to have a selective effect on the ability of the channel to open. Similar results were obtained with D1/S4 (our unpublished observations). Immobilization of D4/S4 has effects both on ability to open and on the kinetics of inactivation. These results agree with previous studies implicating a segregation of function of the S4 segments of the four domains of sodium channels (Chen et al., 1996; Kontis and Goldin, 1997; Kontis et al., 1997; Mitrovic et al., 1998; Cha et al., 1999a). D1/S4 and D2/S4 are relatively exclusively associated with the process of activation, whereas D3/S4 and especially D4/S4 also contribute significantly to the process of fast inactivation. D2/S4 and D4/S4 also play roles in the process of slow inactivation (Fleig et al., 1994; Mitrovic et al., 2000).

One remaining area of controversy is the importance of D4/S4's role in the process of activation. Although every reported mutation of this transmembrane segment influences fast inactivation, both activation and deactivation kinetics are also affected by some mutations (Chahine et al., 1994; Ji et al., 1996; Groome et al., 1999). However, the absolute necessity of D4/S4 movement for activation has been contested (Sheets and Hanck, 1995; Sheets et al., 1999, 2000).

Perhaps the most surprising result of our study is the fact that labeling D4/S4 from the extracellular surface causes a decrease in the rate of fast inactivation and an increase in current amplitude after irradiation, whereas intracellular labeling reduces the ability of the channels to open after irradiation with less effect on inactivation kinetics. The segregation of effects of irradiation was examined in most detail for the residues D4:R1C, which is only accessible to cysteine reagents from the extracellular surface, D4:R4C, which is only accessible from inside, and D4:R3C, which is accessible from both sides of the membrane (Fig. 8). This segregation of the effects of cross-linking was also observed in two other mutants (D4:R2C labeled from the extracellular surface and V1458C, the residue immediately following D4:R4C in the primary sequence, labeled internally, our unpublished observations).

What could be responsible for this spatial segregation of action? One possibility is that the extracellular region of the gating pore is especially important for fast inactivation and, when benzophenone inserts into this

region, it disrupts inactivation gating. This possibility is consistent with the decreasing effects on inactivation of mutations that are located more deeply into the D4/S4 segment from the extracellular surface (Yang et al., 1996; Sheets et al., 1999). Furthermore, a disease-associated mutation, L1433R, near the extracellular end of D4/S3 strongly inhibits the rate of fast inactivation (Ji et al., 1996).

An alternative possibility for explaining the segregation of extracellular and intracellular effects of cross-linking is that depolarization typically might cause the D4/S4 segment to move in multiple steps. The initial movements may be critical for activation gates to open, and subsequent movements may be necessary for efficient inactivation. Cross-linking D4/S4 from the outside may inhibit only the later transitions, whereas cross-linking this S4 segment from the inside inhibits the initial movement after a depolarization. This possibility is testable using a simultaneous measurement of ionic and gating currents in sodium channels, as we have done for our experiments on *Shaker* S4 segments.

This is the first evidence that multiple transitions of a voltage sensor could underlie gating in a sodium channel. This possibility is consistent, however, with the proposed multiple movements of the S4 segments of *Shaker* potassium channels (Bezanilla et al., 1994; Baker et al., 1998). Moreover, the individual transitions of D4/S4 appear to be coupled to different gates. We propose that the sequential movement of D4/S4 in response to a depolarization contributes to the initial opening of the activation gate, followed by the closing of the inactivation gate. This not only helps account for the delay preceding the development of inactivation (Goldman and Schauf, 1972; Bezanilla and Armstrong, 1977), but also provides insight into the efficiency of channel opening during the generation of action potentials.

## APPENDIX

### *Analysis of S4 Cooperativity*

To estimate cooperativity of movement among the S4 segments of *Shaker* potassium channels, we analyzed the normalized reduction of gating and ionic currents in the A359C-BP mutant (Fig. 5). We made the following assumptions for the effects of irradiating S4 segments at a hyperpolarized voltage. (a) All S4 segments are labeled with benzophenone. (b) Immobilization by UV irradiation is a homogeneous Poisson process, and therefore the number of immobilized S4 segments in a channel follows a binomial distribution. (c) Immobilization caused by insertion of a benzophenone-labeled S4 segment completely prevents its ability to carry gating charge. (d) Immobilization of one or more S4 segments of a channel prevents the activation gates from opening. (e) At steady state, UV irradiation has a probability $w = \alpha/(\alpha + \beta)$ of immobilizing a particular S4 segment, and a probability of $1 - w$ of destroying the benzophenone's ability to cross-link (see Scheme I). The probability that an S4 segment is functional at time $t$ during irradiation is $p_{S4}(t)$, which has an exponential time course, as given in Eq. 2. The time course of reduction of ionic current is $p_{S4}^4(t)$. (f) Immobilization of the first S4 segment of a channel may also reduce the gating charge of the other S4 segments by a factor $f_{coop}$, which represents the cooperative fraction of gating charge for each S4 segment. Immobilization of each of the remaining nonimmobilized S4 segments causes a loss of its remaining mobile gating charge.

Let $Fg_j$ ($j = 0,1,...,4$) be the fraction of a channel's gating current if exactly $(4 - j)$ of its S4 segments are immobilized. By the above assumptions,

$$Fg_4 = 1$$
$$Fg_j = j(1 - f_{coop})/4 \qquad j = 0, 1, 2, 3.$$

The total fractional gating current of a channel $Fg_{tot}(t)$ is the sum of $Fg_j$ weighted by the binomial probability $B_j(t)$ that $(4 - j)$ of the channel's S4 segments are immobilized at time $t$, where:

$$B_j(t) = \frac{4!}{j!(4-j)!} p_{S4}^j(t)[1 - p_{S4}(t)]^{4-j}.$$

Therefore,

$$Fg_{tot}(t) = \sum_{j=1}^{4} B_j(t) Fg_j.$$

Note that if $f_{coop} = 0$, then $Fg_{tot}(t) = p_{S4}(t)$. This is the independent case in which immobilization of an S4 segment has no effect on charge movement of other S4 segments, and gating current reduction will exactly track S4 immobilization. At the other extreme, if $f_{coop} = 1$, then $Fg_{tot}(t) = p_{S4}^4(t)$. In this completely cooperative case, the reduction of gating current has the same time course as the reduction of ionic current; i.e., a single immobilization of an S4 segment prevents the others from moving.

The normalized ionic and gating current amplitudes in Fig. 5 were fit simultaneously, using the above equations, by minimization of least squares using a variable metric algorithm. The three parameters for the fit were the time constant of S4 immobilization $\{1/[\lambda(\alpha + \beta)]\}$, $w$, and $f_{coop}$. The best-fit parameters are given in results.

We thank Drs. M. Chahine, A. Melishchuk, and A.L. George for gifts of ion channel mutants and Carol Deutsch, Manuel Covarrubias, and Mike O'Leary for insightful comments on the manuscript.

This study was supported by National Institutes of Health grant AR41691 (R. Horn).

*Submitted: 31 May 2000*
*Revised: 27 July 2000*
*Accepted: 31 July 2000*

REFERENCES

Armstrong, C.M. 1971. Interaction of tetraethylammonium ion derivatives with the potassium channels of giant axons. *J. Gen. Physiol.* 58:413–437.

Armstrong, C.M., and F. Bezanilla. 1977. Inactivation of the sodium channel. II. Gating current experiments. *J. Gen. Physiol.* 70:567–590.

Baker, O.S., H.P. Larsson, L.M. Mannuzzu, and E.Y. Isacoff. 1998. Three transmembrane conformations and sequence-dependent displacement of the S4 domain in shaker $K^+$ channel gating. *Neuron*. 20:1283–1294.

Bezanilla, F. 2000. The voltage sensor in voltage dependent ion channels. *Physiol. Rev.* 80:555–592.

Bezanilla, F., and C.M. Armstrong. 1977. Inactivation of the sodium channel. I. Sodium current experiments. *J. Gen. Physiol.* 70:549–566.

Bezanilla, F., E. Perozo, and E. Stefani. 1994. Gating of *Shaker* $K^+$ channels: II. The components of gating currents and a model of channel activation. *Biophys. J.* 66:1011–1021.

Bénitah, J.P., R. Ranjan, T. Yamagishi, M. Janecki, G.F. Tomaselli, and E. Marban. 1997. Molecular motions within the pore of voltage-dependent sodium channels. *Biophys. J.* 73:603–613.

Catterall, W.A. 1986. Molecular properties of voltage-sensitive sodium channels. *Annu. Rev. Biochem.* 55:953–985.

Cestèle, S., Y.S. Qu, J.C. Rogers, H. Rochat, T. Scheuer, and W.A. Catterall. 1998. Voltage sensor-trapping: enhanced activation of sodium channels by β-scorpion toxin bound to the S3–S4 loop in domain II. *Neuron*. 21:919–931.

Cha, A., and F. Bezanilla. 1997. Characterizing voltage-dependent conformational changes in the *Shaker* $K^+$ channel with fluorescence. *Neuron*. 19:1127–1140.

Cha, A., and F. Bezanilla. 1998. Structural implications of fluorescence quenching in the *Shake*r $K^+$ channel. *J. Gen. Physiol.* 112: 391–408.

Cha, A., P.C. Ruben, A.L. George, Jr., E. Fujimoto, and F. Bezanilla. 1999a. Voltage sensors in domains III and IV, but not I and II, are immobilized by $Na^+$ channel fast inactivation. *Neuron*. 22:73–87.

Cha, A., G.E. Snyder, P.R. Selvin, and F. Bezanilla. 1999b. Atomic scale movement of the voltage-sensing region in a potassium channel measured via spectroscopy. *Nature.* 402:809–813.

Chahine, M., A.L. George, Jr., M. Zhou, S. Ji, W. Sun, R.L. Barchi, and R. Horn. 1994. Sodium channel mutations in paramyotonia congenita uncouple inactivation from activation. *Neuron*. 12:281–294.

Chen, L.-Q., V. Santarelli, R. Horn, and R.G. Kallen. 1996. A unique role for the S4 segment of domain 4 in the inactivation of sodium channels. *J. Gen. Physiol.* 108:549–556.

Del Camino, D., M. Holmgren, Y. Liu, and G. Yellen. 2000. Blocker protection in the pore of a voltage-gated $K^+$ channel and its structural implications. *Nature.* 403:321–325.

Deschênes, I., E. Trottier, and M. Chahine. 1999. Cysteine scanning analysis of the IFM cluster in the inactivation gate of a human heart sodium channel. *Cardiovasc. Res.* 42:521–529.

Dormán, G., and G.D. Prestwich. 1994. Benzophenone photophores in biochemistry. *Biochemistry.* 33:5661–5673.

Fleig, A., J.M. Fitch, A.L. Goldin, M.D. Rayner, J.G. Starkus, and P.C. Ruben. 1994. Point mutations in IIS4 alter activation and inactivation of rat brain IIA Na channels in *Xenopus* oocyte macropatches. *Pflügers Arch.* 427:406–413.

Forkey, J.N., M.E. Quinlan, and Y.E. Goldman. 2000. Protein structural dynamics by single molecule fluorescence polarization. *Prog. Biophys. Mol. Biol.* In press.

French, R.J., E. Prusak-Sochaczewski, G.W. Zamponi, S. Becker, A. Shavantha Kularatna, and R. Horn. 1996. Interactions between a pore-blocking peptide and the voltage sensor of a sodium channel: an electrostatic approach to channel geometry. *Neuron*. 16: 407–413.

Glauner, K.S., L.M. Mannuzzu, C.S. Gandhi, and E.Y. Isacoff. 1999. Spectroscopic mapping of voltage sensor movement in the *Shaker* potassium channel. *Nature*. 402:813–817.

Goldman, L., and C.L. Schauf. 1972. Inactivation of the sodium current in *Myxicola* giant axons: evidence for coupling to the activation process. *J. Gen. Physiol*. 59:659–675.

Gonoi, T., and B. Hille. 1987. Gating of Na channels. Inactivation modifiers discriminate among models. *J. Gen. Physiol.* 89:253–274.

Groome, J.R., E. Fujimoto, A.L. George, Jr., and P.C. Ruben. 1999. Differential effects of homologous S4 mutations in human skeletal muscle sodium channels on deactivation gating from open and inactivated states. *J. Physiol.* 516:687–698.

Holmgren, M., K.S. Shin, and G. Yellen. 1998. The activation gate of a voltage-gated $K^+$ channel can be trapped in the open state by an intersubunit metal bridge. *Neuron*. 21:617–621.

Holmgren, M., P.L. Smith, and G. Yellen. 1997. Trapping of organic blockers by closing of voltage-dependent $K^+$ channels: evidence for a trap door mechanism of activation gating. *J. Gen. Physiol.* 109:527–535.

Hubbell, W.L., D.S. Cafiso, and C. Altenbach. 2000. Monitoring conformational changes with site directed spin labeling. *Nat. Struct. Biol.* In press.

Ji, S., A.L. George, Jr., R. Horn, and R.L. Barchi. 1996. *Paramyotonia congenita* mutations reveal different roles for segments S3 and S4 of domain D4 in hSkM1 sodium channel gating. *J. Gen. Physiol.* 107:183–194.

Kellenberger, S., T. Scheuer, and W.A. Catterall. 1996. Movement of the $Na^+$ channel inactivation gate during inactivation. *J. Biol. Chem.* 271:30971–30979.

Keynes, R.D. 1994. The kinetics of voltage-gated ion channels. *Q. Rev. Biophys.* 27:339–434.

Keynes, R.D., and F. Elinder. 1999. The screw-helical voltage gating of ion channels. *Proc. R. Soc. Lond. B Biol. Sci.* 266:843–852.

Kontis, K.J., and A.L. Goldin. 1997. Sodium channel inactivation is altered by substitution of voltage sensor positive charges. *J. Gen. Physiol.* 110:403–413.

Kontis, K.J., A. Rounaghi, and A.L. Goldin. 1997. Sodium channel activation gating is affected by substitutions of voltage sensor positive charges in all four domains. *J. Gen. Physiol.* 110:391–401.

Ledwell, J.L., and R.W. Aldrich. 1999. Mutations in the S4 region isolate the final voltage-dependent cooperative step in potassium channel activation. *J. Gen. Physiol.* 113:389–414.

Liu, Y., M. Holmgren, M.E. Jurman, and G. Yellen. 1997. Gated access to the pore of a voltage-dependent $K^+$ channel. *Neuron*. 19: 175–184.

Liu, Y., M.E. Jurman, and G. Yellen. 1996. Dynamic rearrangement of the outer mouth of a $K^+$ channel during gating. *Neuron*. 16: 859–867.

Mannuzzu, L.M., and E.Y. Isacoff. 2000. Independence and cooperativity in rearrangements of a potassium channel voltage sensor revealed by single subunit fluorescence. *J. Gen. Physiol.* 115:257–268.

Mannuzzu, L.M., M.M. Moronne, and E.Y. Isacoff. 1996. Direct physical measure of conformational rearrangement underlying potassium channel gating. *Science.* 271:213–216.

Melishchuk, A., A. Loboda, and C.M. Armstrong. 1998. Loss of *Shaker* K channel conductance in 0 $K^+$ solutions: role of the volt-

age sensor. *Biophys. J.* 75:1828–1835.

Mitrovic, N., A.L. George, Jr., and R. Horn. 1998. Independent versus coupled inactivation in sodium channels: role of the domain 2 S4 segment. *J. Gen. Physiol.* 111:451–462.

Mitrovic, N., A.L. George, Jr., and R. Horn. 2000. Role of domain 4 in sodium channel slow inactivation. *J. Gen. Physiol.* 115:707–718.

Ottemann, K.M., W. Xiao, Y.-K. Shin, and D.E. Koshland. 1999. A piston model for transmembrane signaling of the aspartate receptor. *Science.* 285:1751–1754.

Patton, D.E., J.W. West, W.A. Catterall, and A.L. Goldin. 1992. Amino acid residues required for fast $Na^+$-channel inactivation: charge neutralizations and deletions in the III-IV linker. *Proc. Natl. Acad. Sci. USA.* 89:10905–10909.

Perozo, E., D.M. Cortes, and L.G. Cuello. 1999. Structural rearrangements underlying $K^+$-channel activation gating. *Science.* 285:73–78.

Rohl, C.A., F.A. Boeckman, C. Baker, T. Scheuer, W.A. Catterall, and R.E. Klevit. 1999. Solution structure of the sodium channel inactivation gate. *Biochemistry.* 38:855–861.

Schoppa, N.E., and F.J. Sigworth. 1998. Activation of *Shaker* potassium channels III. An activation gating model for wild-type and V2 mutant channels. *J. Gen. Physiol.* 111:313–342.

Sheets, M.F., and D.A. Hanck. 1995. Voltage-dependent open-state inactivation of cardiac sodium channels: gating current studies with Anthopleurin-A toxin. *J. Gen. Physiol.* 106:617–640.

Sheets, M.F., J.W. Kyle, and D.A. Hanck. 2000. The role of the putative inactivation lid in sodium channel gating current immobilization. *J. Gen. Physiol.* 115:609–619.

Sheets, M.F., J.W. Kyle, R.G. Kallen, and D.A. Hanck. 1999. The Na channel voltage sensor associated with inactivation is localized to the external charged residues of domain IV, S4. *Biophys. J.* 77: 747–757.

Sigworth, F.J. 1994. Voltage gating of ion channels. *Q. Rev. Biophys.* 27:1–40.

Slatin, S.L., X.-Q. Qiu, K.S. Jakes, and A. Finkelstein. 1994. Identification of a translocated protein segment in a voltage-dependent channel. *Nature.* 371:158–161.

Smith-Maxwell, C.J., J.L. Ledwell, and R.W. Aldrich. 1998b. Role of the S4 in cooperativity of voltage-dependent potassium channel activation. *J. Gen. Physiol.* 111:399–420.

Smith-Maxwell, C.J., J.L. Ledwell, and R.W. Aldrich. 1998a. Uncharged S4 residues and cooperativity in voltage-dependent potassium channel activation. *J. Gen. Physiol.* 111:421–439.

Subbiah, S. 1996. Protein Motions. Springer Publishing Co., Inc., New York, NY. 1–213.

Swartz, K.J., and R. MacKinnon. 1997a. Hanatoxin modifies the gating of a voltage-dependent $K^+$ channel through multiple binding sites. *Neuron.* 18:665–673.

Swartz, K.J., and R. MacKinnon. 1997b. Mapping the receptor rite for Hanatoxin, a gating modifier of voltage-dependent $K^+$ channels. *Neuron.* 18:675–682.

Tsushima, R.G., R.A. Li, and P.H. Backx. 1997. P-loop flexibility in $Na^+$ channel pores revealed by single- and double-cysteine replacements. *J. Gen. Physiol.* 110:59–72.

Tytgat, J., and P. Hess. 1992. Evidence for cooperative interactions in potassium channel gating. *Nature.* 359:420–423.

Vale, R.D., and R.A. Milligan. 2000. The way things move: looking under the hood of molecular motor proteins. *Science.* 288:88–95.

Vassilev, P.M., T. Scheuer, and W.A. Catterall. 1988. Identification of an intracellular peptide segment involved in sodium channel inactivation. *Science.* 241:1658–1661.

Weiss, S. 1999. Fluorescence spectroscopy of single biomolecules. *Science.* 283:1676–1683.

West, J.W., D.E. Patton, T. Scheuer, Y. Wang, A.L. Goldin, and W.A. Catterall. 1992. A cluster of hydrophobic amino acid residues required for fast $Na^+$-channel inactivation. *Proc. Natl. Acad. Sci. USA.* 89:10910–10914.

Yang, N., A.L. George, Jr., and R. Horn. 1996. Molecular basis of charge movement in voltage-gated sodium channels. *Neuron.* 16: 113–122.

Yang, N., and R. Horn. 1995. Evidence for voltage-dependent S4 movement in sodium channels. *Neuron.* 15:213–218.

Yellen, G. 1998. The moving parts of voltage-gated ion channels. *Q. Rev. Biophys.* 31:239–295.

Zhan, H., S. Choe, P.D. Huynh, A. Finkelstein, D. Eisenberg, and R.J. Collier. 1994. Dynamic transitions of the transmembrane domain of diphtheria toxin: disulfide trapping and fluorescence proximity studies. *Biochemistry.* 33:11254–11263.